

Geophysical Research Letters

RESEARCH LETTER

10.1029/2018GL080098

Key Points:

- A monsoon-enhanced subtropical high dictates a westward shift of Atlantic tropical cyclones in observations and in a statistical track model
- Interannual variations in steering effects are due to internal Indian monsoon variability, independent of ENSO
- Previous changes in steering and landfall probability attributed to ENSO need to account for ENSO's correlation to the Indian monsoon

Supporting Information:

- Supporting Information S1

Correspondence to:

P. Kelly,
patrick.kelly@pnnl.gov

Citation:

Kelly, P., Leung, L. R., Balaguru, K., Xu, W., Mapes, B., & Soden, B. (2018). Shape of Atlantic tropical cyclone tracks and the Indian monsoon. *Geophysical Research Letters*, 45, 10,746–10,755. <https://doi.org/10.1029/2018GL080098>

Received 17 AUG 2018

Accepted 24 SEP 2018

Accepted article online 1 OCT 2018

Published online 10 OCT 2018

Shape of Atlantic Tropical Cyclone Tracks and the Indian Monsoon

Patrick Kelly¹ , L. Ruby Leung¹ , Karthik Balaguru¹ , Wenwei Xu¹, Brian Mapes² , and Brian Soden² 

¹Atmospheric Sciences and Global Change Division, Pacific Northwest National Laboratory, Richland, WA, USA, ²Rosenstiel School of Marine and Atmospheric Science, University of Miami, Miami, FL, USA

Abstract We find a significant enhancement of the North Atlantic subtropical high on interannual timescales (1970–2016) concurrently linked to an anomalously strong Indian monsoon in September. Consistent with a stronger North Atlantic subtropical high, enhanced anticyclonic flow and subtropical easterlies in the eastern Atlantic basin are found during strong monsoon years. Observational regression analysis combined with a statistical track model are used to assess the influence of these monsoon-linked wind variations on Atlantic tropical cyclone (TC) tracks originating in the main development region. When controlling for effects of El Niño–Southern Oscillation (ENSO), a westward shift of TC tracks is shown to be robustly correlated to internal monsoon variability in September. This work highlights variability of the Indian monsoon as an additional constraint on Atlantic TCs, with increased landfall probability during a strong monsoon. Previous attribution of similar steering effects to ENSO need to be reconsidered to account for ENSO's correlation with the monsoon.

Plain Language Summary Variations of tropical cyclone or hurricane impacts (such as landfall probability) depend on steering effects, in addition to effects that govern their intensity or frequency. These steering effects are a key factor governing *where hurricanes go* after they form. For the first time, we use observations and modeling evidence to show that year-to-year variations of tropical cyclone steering effects in the Atlantic are related to the Indian monsoon. This is because monsoon heating from rainfall drives the large-scale counterclockwise circulation in the Atlantic known as the North Atlantic subtropical high. When the monsoon is stronger, the subtropical high is stronger, which means enhanced flow from the east steers tropical cyclones more strongly westward in the Atlantic. An implication of these results is an increase likelihood of landfalling hurricane events during a strong monsoon, after controlling for other factors. These results also challenge a prevailing notion that La Niña events cause more landfalling hurricanes due to steering changes. Our analysis suggests that causality inference may partially be happenstance, since a strong Indian monsoon often occurs during La Niña events.

1. Introduction

The steering of tropical cyclone (TC) tracks is primarily controlled by the environmental flow in which they are embedded, plus a systematic beta drift owing to the interaction of the storm's vortex with the Earth's background vorticity field (Holland, 1983). Understanding environmental steering flow changes is thus essential to understanding differences in TC tracks. In the North Atlantic basin, the location and intensity of the North Atlantic subtropical high (NASH) directly modulates TC tracks (Colbert & Soden, 2012; Elsner et al., 2000; Kossin et al., 2010).

Coherent changes in TC track density can be linked to known *modes* of climate variability to help explain variations in TC tracks on interannual timescales and longer (e.g., Xie et al., 2005). But steering effects need to be carefully distinguished from variations in genesis location, storm frequency, and/or storm duration when diagnosing and interpreting variations in TC tracks. These other TC statistics may arise from a distinct set of physical processes but can be conflated in any particular measure of storm density. In this study, we are specifically interested in the role of steering flow variations on Atlantic TC tracks on interannual timescales in the postsatellite record (1970–2016).

El Niño–Southern Oscillation (ENSO) is particularly relevant to changes in North Atlantic TC tracks on interannual timescales. La Niña events have been associated with more landfalling Atlantic TCs (Bove et al.,

1998; Pielke & Landsea, 1999), consistent with a strengthening of the NASH and its associated changes in steering flow (Colbert & Soden, 2012). These ENSO-related steering impacts are in addition to the well-known influence of ENSO on basinwide TC activity in the North Atlantic due to wind shear variability (Gray, 1984; Shapiro, 1987) and tropical stability factors (Tang & Neelin, 2004).

Other non-ENSO sources of climate variability may be relevant to Atlantic TC track changes too. The Atlantic Meridional Mode has been shown to modulate interannual and decadal variations in Atlantic TC tracks (Vimont & Kossin, 2007), but this may be due to variations in genesis location rather than pure steering flow differences (Colbert & Soden, 2012). Also, attribution of TC variability to the Atlantic Meridional Mode is further conflated by the concurrent phase of ENSO (Patricola et al., 2014). The North Atlantic Oscillation (NAO) is another likely candidate, as it involves a basin-scale seesaw of sea level pressure (SLP; Hurrell et al., 2003). Several studies linked NAO phase to the shape of Atlantic TC tracks and subsequent landfall probability (Elsner, 2003; Elsner & Bossak, 2001; Elsner et al., 2000). More recent analysis, however, suggests that NAO-induced steering impacts may only be relevant to a small subsample of observed TCs, with no significant relationship to TCs originating in the main development region or MDR (Colbert & Soden, 2012; Kossin et al., 2010).

In relating known sources of climate variability to Atlantic TC tracks, we have found no mention of the Indian monsoon in the scientific literature. This may seem surprising, given the well-documented role of the NASH on TC steering (e.g., Colbert & Soden, 2012; Elsner et al., 2000; Kossin et al., 2010), and the well-documented role of the Indian monsoon on the maintenance and variability of the NASH. For instance, remote diabatic heating over the continental Indian monsoon region has been shown to drive the summertime circulation in the Atlantic, owing to adiabatic descent as the background westerlies interact with the anomalous Rossby wave pattern west of the heating (Rodwell & Hoskins, 1996, 2001). The Indian monsoon can also influence the NASH remotely through downstream (eastward) energy propagation (e.g., Chen et al., 2001) and via eddy-mediated mean flow changes (Kelly & Mapes, 2011, 2013).

In this study, we revisit the connection of ENSO to Atlantic TC tracks via the proximate steering influence of the NASH, but with the recognition that ENSO is negatively correlated to the Indian monsoon (Ju & Slingo, 1995; Shukla & Paolino, 1983; Webster & Yang, 1992). In a partial correlation accounting for both ENSO and monsoon, we find a significant westward shift of TC tracks during strong monsoon years, consistent with steering effects of a monsoon-enhanced NASH. Our findings indicate that Atlantic TC steering impacts previously ascribed to ENSO (e.g., Colbert & Soden, 2012) need to account for ENSO's partial collinearity with the Indian monsoon, which clarifies that monsoon variability is a significant driver of steering changes.

2. Linking TC Variations to the Indian Monsoon

In relating interannual variations of TC activity to the monsoon, we primarily use the Indian monsoon index or IMI (Wang & Fan, 1999) as a proxy for monsoon intensity, but other circulation indices are also considered (section 6) and shown to give consistent results. Significant differences in TC tracks are seen during September when composited on anomalously high ($\geq 33\%$) IMI years. Figure 1 shows 10-day tracks of named storms initiating within the MDR, for high IMI years (blue) and all years (1970–2016; black/gray). Thick lines indicate the average track for each group, and annotations show the genesis locations and the respective ± 1 standard deviation error at the 7- and 10-day life stages. Nonoverlapping ovals indicate a significant westward shift in the trajectory of long-lived (≥ 10 day) MDR storms during high IMI years, despite similar mean genesis points (Figure 1a). Contours of track density differences give a complementary picture to these mean TC track changes (Figure 1b). Here TC density is defined as 6-hourly event counts summed within $5^\circ \times 5^\circ$ longitude by latitude bins. When all (i.e., lifetime ≥ 6 hr) MDR storms in the HURDAT2 database are considered, univariate regression analysis with the IMI as the predictor shows a significant enhancement of TC density in the western Atlantic. Identical composite/regression analysis applied to other measures of monsoon intensity yield similar results (Figure S1 in the supporting information).

Since the NASH is the dominant low-level synoptic feature in this region in summer, its variability has a strong impact on the steering flow of TCs. An anomalously strong NASH and anticyclonic steering pattern in the eastern Atlantic are found when SLP and winds are regressed on the IMI (Figure 1c). Stronger subtropical easterlies in the eastern Atlantic imply that storms that form in the MDR would tend to be advected more strongly westward, an interpretation consistent with the increase in TC density west of 50°W (Figure 1b).

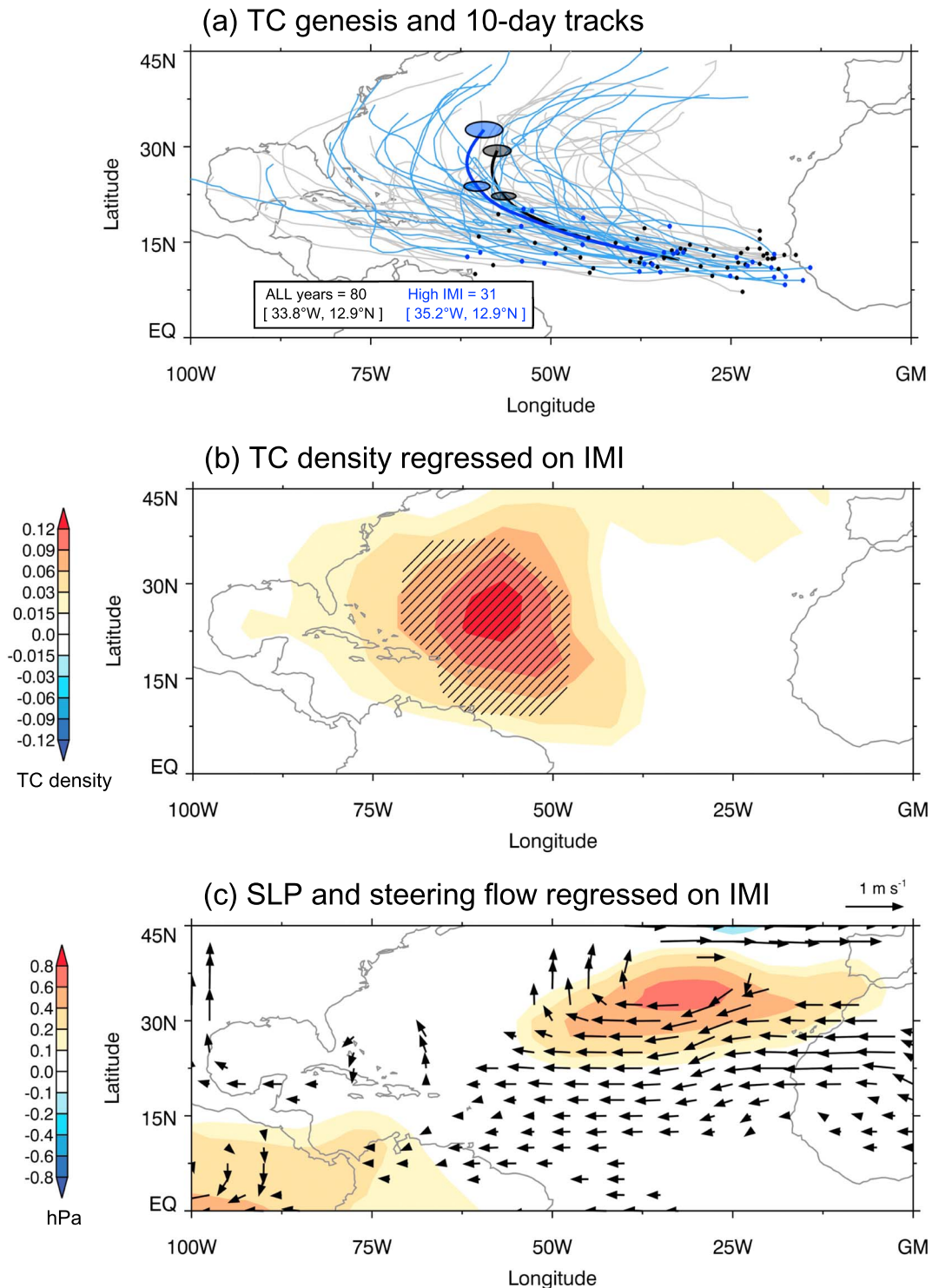


Figure 1. Enhanced tropical cyclones (TCs) in the western Atlantic with a stronger Indian monsoon. (a) September 10-day tracks for main development region TCs composited over high Indian monsoon index (IMI) years (upper 33%, blue) and all years (gray/black) from 1970 to 2016 with thick lines indicating the average track. Small circles indicate genesis points with high IMI in blue, and ovals indicate ± 1 standard deviation error at the 7- and 10-day mark. Inset shows mean genesis location and sample size. (b) Univariate regression coefficients of September TC density on the contemporaneous IMI for main development region storms, where TC density units is counts per 6 hr per $5^\circ \times 5^\circ$ grid box per unit increase. (c) Univariate regression coefficients of September sea level pressure (SLP) (contours) and steering flow (arrows) on the contemporaneous IMI. Crosshatching in (b) indicates the 95% confidence level using a bootstrap significance test, with only significant values plotted in (c).

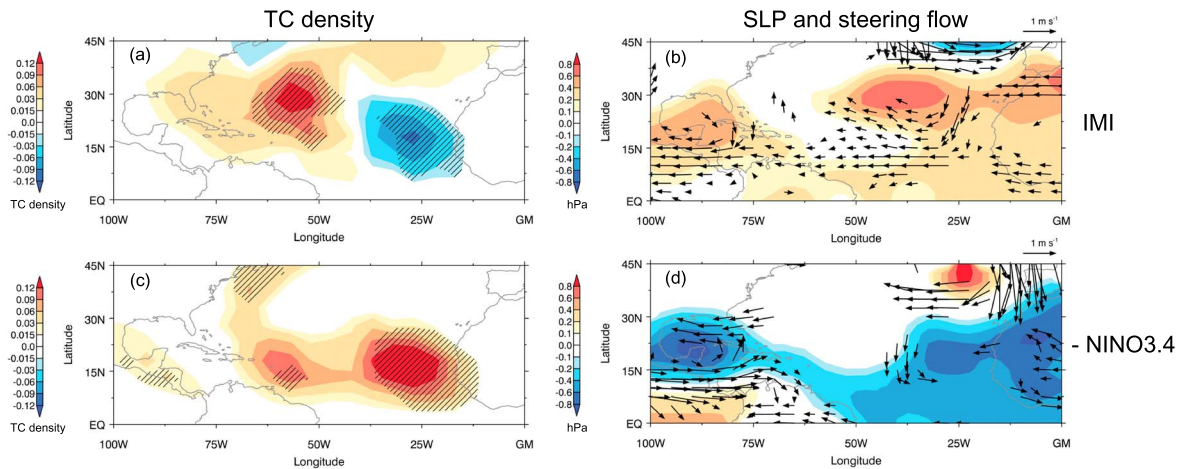


Figure 2. A westward shift of tropical cyclones (TCs) with a stronger Indian monsoon. Partial regression coefficients of TC density (a, c) and sea level pressure (SLP) and steering flow (b, d) for Indian monsoon index (IMI; a and b) and $-NINO3.4$ (c and d) as the joint predictors for the month of September (1970–2016). The $NINO3.4$ index is multiplied by (-1) for visual convenience to identify areas of compensation from correlated predictors. TC data are from HURDAT2 and wind and SLP data are from NCEP-GR1. Only storms with genesis in the main development region are included. Crosshatching significance convention as in Figure 1.

But changes in TC density due to pure steering changes imply a zonal *displacement* or east-west dipole of TC density. We show next that the lack of a corresponding decrease in TC density in the eastern Atlantic (Figure 1b) is due to destructive interference between the monsoon and ENSO signals.

3. Separating Monsoon and ENSO Effects on TC Tracks

The Indian monsoon and ENSO are negatively correlated on interannual timescales (Ju & Slingo, 1995; Shukla & Paolino, 1983; Webster & Yang, 1992), although the relationship has varied through time and is relatively weak in recent decades (Kumar et al., 1999). Previous studies found La Niña years to be associated with more landfalling Atlantic TCs (Bove et al., 1998; Pielke & Landsea, 1999). That result is consistent with enhanced TC density in the western Atlantic during strong monsoon years found here (Figure 1), given the negative correlation between monsoon and ENSO.

Are the aforementioned TC and steering flow differences (Figure 1) truly driven by monsoon variations then, or are they merely a reflection of ENSO-linked variability? To address this question, we expand on the univariate regression analysis above by using joint (or partial) linear regression. This simple but effective statistical technique optimally partitions TC variance between two different but correlated predictors (section 6).

Previous studies (e.g., Boudreault et al., 2017; Hall & Yonekura, 2013; Kozar et al., 2012) have used similar multiple predictor regression techniques to assess historical Atlantic TC variations but have not explicitly considered the Indian monsoon as a constraint.

Figure 2 shows the partial regression coefficients of TC density, SLP, and steering flow for the IMI and the negative of $NINO3.4$. We multiply $NINO3.4$ by (-1) here for visualization convenience, to highlight the compensation in the eastern Atlantic. For a given $-NINO3.4$ value, regression of TC density on the IMI (Figure 2a) shows a clear dipole structure with negative values in the eastern Atlantic and positive values in the western Atlantic, consistent with enhanced anticyclonic steering by the NASH (Figure 2b). Alternatively, for a given IMI value, regression of TC density on $-NINO3.4$ shows a single-signed increase in TC activity, consistent with the well-known influence of ENSO on *basinwide* TC activity (e.g., Gray, 1984; Shapiro, 1987). The significant increase in TC density in the western Atlantic ($\sim 55^\circ W$, $25^\circ N$) for MDR storms is similar in both univariate regression on the IMI (Figure 1b), and partial regression with the IMI and $-NINO3.4$ as joint predictors (Figure 2a). In contrast, joint regression of TCs on the IMI and $-NINO3.4$ offset each other in the eastern Atlantic (Figures 2a and 2c), explaining the lack of negative anomalies in the eastern Atlantic in Figure 1b.

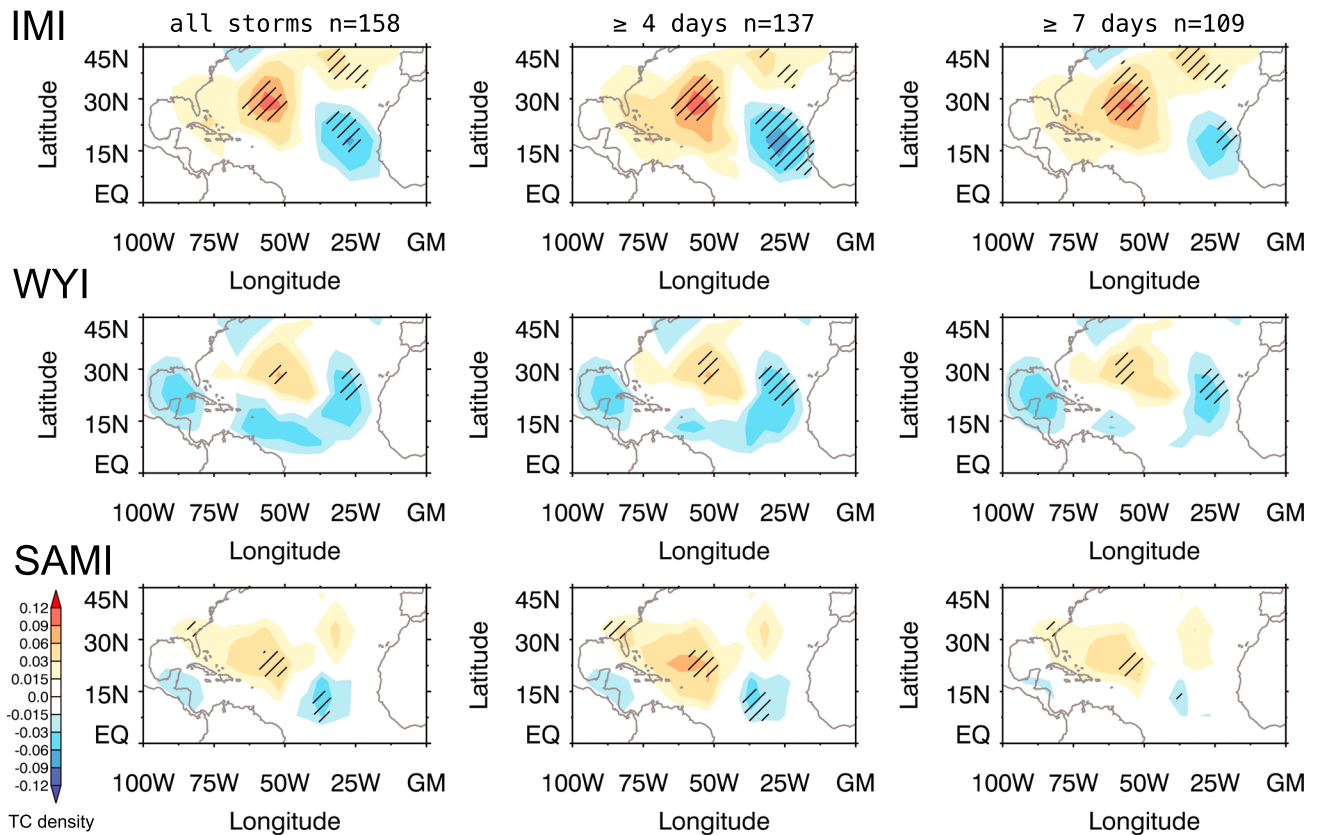


Figure 3. Robust monsoon steering effects independent of El Niño–Southern Oscillation. Regression coefficient of tropical cyclone (TC) density on various circulation indices (rows) of the Indian monsoon for September (1970–2016) after linearly removing the El Niño–Southern Oscillation signal (section 6), where TC density units is event counts per 6 hr per $5^\circ \times 5^\circ$ grid box per unit increase. TC density is further stratified by storm duration (columns). Only storms with genesis in the main development region are included. Crosshatching significance convention as in Figure 1.

Other measures of the monsoon give similar results (Figure 3), namely, the Webster–Yang index (WYI; Webster & Yang, 1992) and the South Asian monsoon index (SAMI; Goswami et al., 1999). The results are also robust to substratification of TC data by storm duration (columns in Figure 3), since it too may affect TC density composites. The signal even remains in a successive decomposition with ENSO privileged. That is, when we first remove TC variability linearly related to NINO3.4 (section 6), a stronger monsoon still significantly predicts a westward shift of TC activity for MDR storms (Figure 3). In this successive decomposition with ENSO removed, we see near-equal concentration of positive and negative anomalies implying a *displacement* in TCs related to *steering* impacts (Figure 3), whose eastern lobe is compensated by the basinwide changes in TC *frequency* related to ENSO (as shown in Figure 2c). Again, this relationship is consistent across various measure of monsoon intensity and is independent of TC lifespan. Other measures of ENSO aside from NINO3.4 were also considered. The principal monsoon TC steering signal is robust when variance from different ENSO types are removed (see Figure S7), with no discernible difference if events in the Central or East Pacific are emphasized, consistent with the common impact on TC frequency by different flavors of ENSO (Patricola et al., 2016).

4. Simulations Using a TC Track Model

To further isolate steering effects from genesis location effects, a statistical TC track model (developed following Emanuel et al., 2006) is used to test our observational inference that monsoon-related steering flow variations cause a realistic westward shift of Atlantic MDR storms. A total of seven sets of simulations were performed (six experiments and one control; see section 6). In each set, the model integrates a total of 7,000 synthetic tracks originating from the same genesis points in the MDR. Differences in track statistics thus arise solely from differences in the steering flow. A realistic westward shift in TC tracks is found when

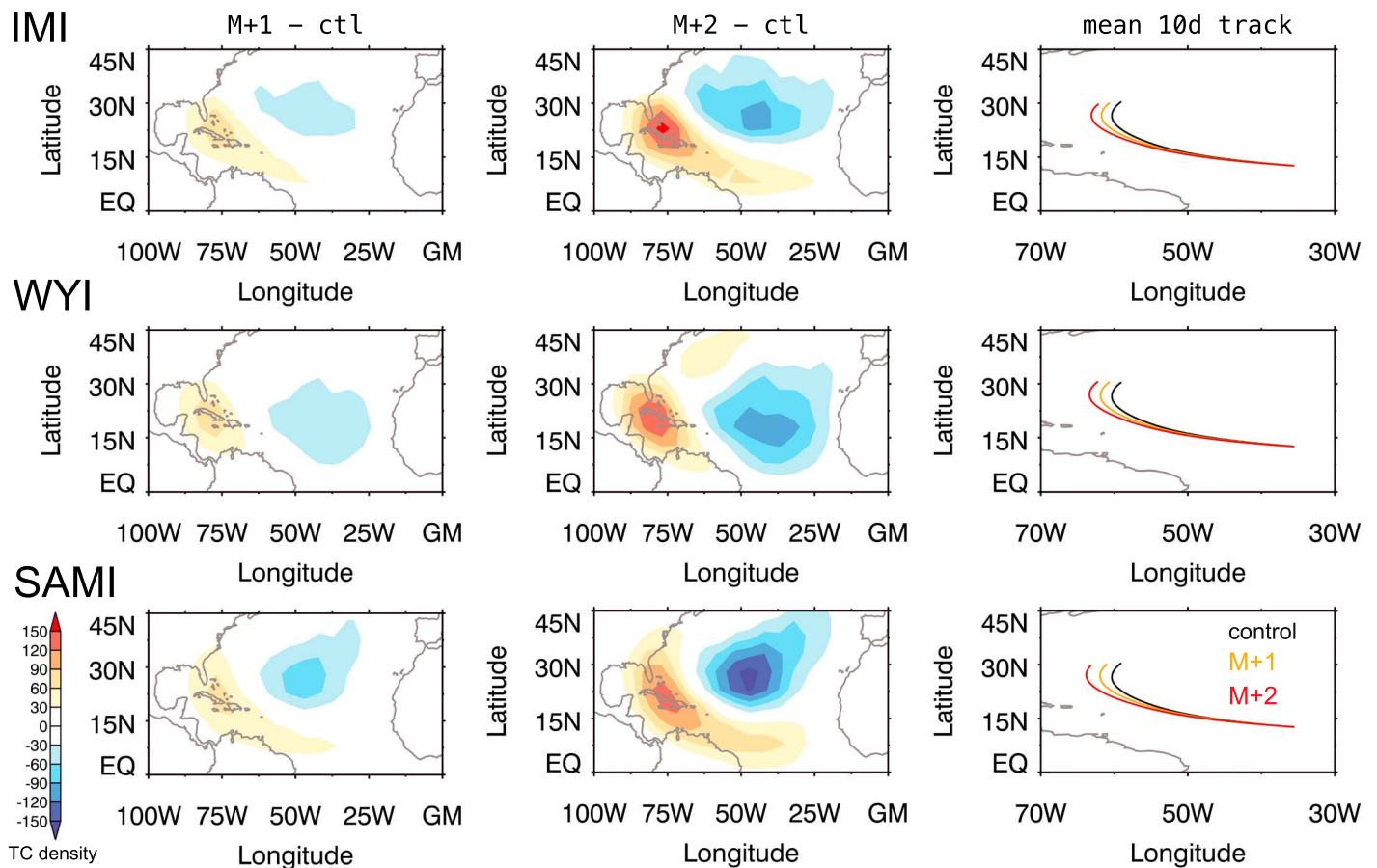


Figure 4. Realistic shift of model tropical cyclone (TC) tracks with stronger monsoon. Track model TC density difference for experiment minus control where experiment is +1 (left column) and +2 (middle column) standard deviation of the indicated monsoon index (rows), and mean 10-day track for the control and monsoon perturbation experiments (right column). TC density in units of event counts per $5^\circ \times 5^\circ$ grid box. All simulations used 7,000 synthetic tracks with genesis points uniformly seeded in the main development region. See section 6 for details. IMI = Indian monsoon index; WYI = Webster-Yang index; SAMI = South Asian monsoon index.

monsoon-regressed wind anomalies are added to the background steering flow (Figure 4). The model response is characterized by a robust increase in TCs in the western Atlantic and corresponding decrease in the eastern Atlantic, the fingerprint of a steering effect. The magnitude of the response is approximately linear given $M + 1$ and $M + 2$ scalings of the monsoon-regressed wind anomalies, equivalent to plus 1 and 2 standard deviations of the monsoon. The dipole pattern of the model response is highly consistent across all monsoon indices, as in observations (Figure 3). The pattern of the model response is displaced slightly westward with respect to observed anomalies, however. This discrepancy appears linked to the model's underlying (mean) westward bias in TC density (Figure S6).

5. Summary and Discussion

Interannual variations of TC impacts (such as landfall probability) depend on steering effects, in addition to effects that govern TC intensity or frequency. Here we find that interannual variations of the Indian monsoon (indexed by various measures) are correlated with enhanced TC activity in the western Atlantic (Figure 1). Even when linear correlations with ENSO are removed, this enhancement in TC activity is present and is indicative of a westward shift in TC activity corresponding to a stronger monsoon, separate from ENSO's basin-wide effects (Figures 2 and 3). The westward shift in TC tracks is consistent with steering impacts from a stronger NASH and stronger subtropical easterlies (Figures 1c and 2b). Attribution of the pattern to steering effects is bolstered by results from a statistical track model forced by monsoon-regressed wind anomalies, which yields a similar response to these observations (Figure 4).

Our results apply principally to September, the peak in Atlantic TC activity, and to MDR storms in particular. However, the relationship appears to also hold when all genesis locations and the broader TC season (e.g., August–October) are considered, albeit with less clarity and consistency (Figures S3 and S4). We suspect this weakening of the signal stems (at least in part) from the asynchronous relationship between the Indian monsoon and Atlantic TC seasonal cycles. While TCs peak in September, the climatological monsoon is decaying at this time. Anomalies in monsoon intensity during September are not simply a reflection of anomalies in the broad seasonal mean monsoon (Figure S5). Rather, anomalous precipitation during September on interannual timescales appears linked to the cumulative result of northward propagating low-frequency intraseasonal anomalies (Figure S5). Since the Madden-Julian Oscillation (MJO) is known to modulate Atlantic TCs (e.g., Belanger et al., 2010; Klotzbach, 2010; Mo, 2000) and is also partially correlated with monsoonal intraseasonal variability (e.g., Waliser, 2006), further work is needed to tease apart and attribute the mechanisms of intraseasonal variability on Atlantic TCs. Our interannual signal could be a form of aliasing of a fundamentally intraseasonal signal, since 1 month fails to average over entire intraseasonal cycles.

By identifying internal variability of the Indian monsoon as a constraint, this work extends an already rich literature connecting Atlantic TCs to modes of climate variability, with effects both local and nonlocal. For instance, apparent steering related impacts previously ascribed to ENSO (e.g., Colbert & Soden, 2012) may need to be reconsidered to account for ENSO's collinearity with the Indian monsoon. Typically, remote responses to monsoon heating are ascribed to propagating Rossby waves (e.g., Chen et al., 2001; Rodwell & Hoskins, 2001), which can make very long-distance effects like Atlantic basin impacts delicately mean flow dependent. However, eddy effects on zonal mean momentum, mediated by the shape of the monsoon-driven Tibetan High (Kelly & Mapes, 2011, 2013), provide a more direct and inherently global mechanism of impact that might also be relevant here.

The Indian monsoon has a sharp onset in late May and has largely decayed by September in the present climate. Climate model projections suggest monsoon precipitation will increase and the monsoon withdrawal may occur later under future warming (Lee & Wang, 2014). These changes are expected to occur alongside a robust westward shift in the NASH circulation (Shaw & Voigt, 2015). Whether causally related or coincidental, these changes may have significant implications for the steering of Atlantic TCs in the future. Alternatively, our results provide another possible mechanism for interpreting paleo proxies of Atlantic TC variations in past climates (e.g., Elsner et al., 2000), since a stronger monsoon during the mid-Holocene similarly drove robust steering changes of the NASH (Kelly et al., 2018).

Despite enormous efforts, operational forecasts of Indian monsoon rainfall have been poor recently due to climate change (Wang et al., 2015). Improved prediction of the monsoon is critically important not just locally but also potentially for remote high impact events as studied here. Our results imply that better understanding of the monsoon and its variability—now and into the future—may lead to improved predictability of Atlantic TC activity, with implications on landfall probability in particular. It is hoped that the present work motivates future study of monsoon-linked TC variability in the Atlantic, from subseasonal to climate change timescales.

6. Methods

6.1. HURDAT2 and Steering Flow Data

TC best track data comes from the revised Atlantic hurricane database (HURDAT2: <http://www.aoml.noaa.gov/hrd/hurdat/hurdat2.html>). We focus on storms that form in the MDR, defined here as the area between 14–65°W and 7–20°N. We only use data from the postsatellite era (1970–2016) to minimize uncertainty in the historical record (Landsea & Franklin, 2013) since we are interested in basinwide track statistics. We make no delineation of TCs based on intensity and use track data from all individual storm ≥ 6 -hr duration in HURDAT2. Substratification of TCs by storm duration does not change the results or conclusions therefrom (Figure 3). We focus on the month of September, since it is the peak month of climatological Atlantic TC activity (Landsea, 1993). In aggregating storm statistics for the month of September, storms that also span the calendar month of August or October are counted here as *September* storms, as we initially make no artificial truncation of storm tracks in Figure 2. This choice is examined in detail and the results are shown to be independent of methodological choices in counting statistics (Figure S2). SLP and steering flow data come from

monthly mean NCEP-GR1 data (Kalnay et al., 1996) for the period 1970–2016. Steering vectors are defined as the weighted mean of winds at 200 and 850 hPa:

$$\mathbf{V}_{\text{steering}} = \alpha \mathbf{V}_{850} + (1 - \alpha) \mathbf{V}_{200}, \quad (1)$$

where $\alpha = 0.8$.

6.2. Monsoon and ENSO Indices

We use NINO3.4 index (Trenberth, 1997) calculated as anomalies from the HadISST1 data set (Rayner et al., 2003) provided by National Oceanic and Atmospheric Administration Earth System Research Laboratory Physical Science Division. We use several circulation indices of the monsoon, including the IMI (Wang & Fan, 1999), WYI (Webster & Yang, 1992), and the SAMI (Goswami et al., 1999). NCEP-GR1 (Kalnay et al., 1996) monthly mean data spanning years 1970–2016 are used to calculate all monsoon indices.

In relating the monsoon and ENSO to Atlantic TCs on interannual timescales, we consider contemporaneous correlations during September in our regression and composite analysis. To parse the effects of collinearity of monsoon-ENSO (Table S1), we use joint (partial) linear regression in Figure 2 and postulate the following form:

$$Y = \beta_1 M + \beta_2 N_{3.4} + \varepsilon, \quad (2)$$

where $\beta_1 = \left. \frac{\partial Y}{\partial M} \right|_{N_{3.4}}$ and $\beta_2 = \left. \frac{\partial Y}{\partial N_{3.4}} \right|_M$. In (2), Y is the target variable of interest (TC count, SLP, or steering flow); M and $N_{3.4}$ are the IMI and NINO3.4 index, respectively; and ε is the residual. Elsewhere in the text (e.g., Figures 3 and 4), we remove the ENSO signal from the target variable *before* regressing on the monsoon in order to deconvolve their covariance. In this successive decomposition, we subtract variability linearly related to ENSO, acknowledging it may not completely remove the ENSO signal (Compo & Sardeshmukh, 2010), as

$$Y = X - \beta N_{3.4}, \quad (3)$$

where X is the original observed data and β is the regression coefficient projected onto NINO3.4. We then separately regress Y onto the various monsoon indices (IMI, WYI, and SAMI). A bootstrap method is used to test for significance of all regression coefficients. The data sample is divided in half for 100 random subsamples and the regression calculations are repeated. Regions where 95% of the random integrations have the same sign are counted as statistically significant.

6.3. TC Track Model

We use simulations from a statistical TC track model (Emanuel et al., 2006) to test our inference-based hypothesis that a stronger Indian monsoon is linked to a westward shift in Atlantic TC tracks due to steering changes. We generated tracks based on a synthetic time series of the wind (following Appendix B in Emanuel et al., 2006). The reader is referred to the supplement section of that reference (ftp://18.83.0.193/ftp/pub/emanuel/PAPERS/hurr_risk_suppl.pdf) for a detailed description of the model. Briefly, the track model generates storms as a random draw from the historical density distribution of MDR genesis locations and times for September (1970–2016). The tracks propagate according to a weighted average of the ambient flow at 850 and 200 hPa, plus a beta-drift correction. Instead of using a constant beta-drift term as in Emanuel et al. (2006), we followed the approach of Wu and Wang (2004) and Zhao et al. (2009) and calculated beta drift as temporally averaged but spatially varying vectors in the North Atlantic basin. To terminate the tracks, we assumed the lifespan of MDR storms in September as a normal distribution and calculated the mean and standard deviation from the historical tracks in HURDAT2 (9.3 and 4.8 days, respectively). Then we used these values to constrain random lifespans for each synthetic track so that the bulk TC lifespan statistics of the synthetic tracks are realistic.

A total of seven sets of simulations are performed (one control and six experiments). For each simulation, the model integrated a total of 7,000 tracks originating from the same set of genesis points. Differences in track statistics thus arise solely from differences in steering flow. The environmental steering flow in the North Atlantic basin is modeled at each level (200 and 850 hPa) in the control simulation (CTL) as

$$\mathbf{V}_{\text{ctl}} = \bar{\mathbf{V}}_{\text{obs}} + \sqrt{\bar{\mathbf{V}}_{\text{obs}}^2} \mathbf{F} \quad , \quad (4)$$

where $\bar{\mathbf{V}}_{\text{obs}}$ is the September climatological (1970–2016 average) vector wind from NCEP-GR1 and $\bar{\mathbf{V}}_{\text{obs}}^2$ is the interannual variance from this September climatology.

The vector \mathbf{F} is a Fourier series with random phase and represents large-scale turbulent motions (see equations S1–S4 in Emanuel et al., 2006, for full details). The climatology of synthetic tracks modeled with (4) is compared to observations in Figure S6.

We then performed a series of six experiments (EXP), where the monsoon-regressed wind anomalies associated with internal monsoon variability are added to (4):

$$\mathbf{V}_{\text{exp}} = \bar{\mathbf{V}}_{\text{pert}} + \sqrt{\bar{\mathbf{V}}_{\text{pert}}^2} \mathbf{F} \quad , \quad (5)$$

where

$$\mathbf{V}_{\text{pert}} = (\mathbf{V}_{\text{obs}} + \beta M) \quad , \quad (6)$$

and β is the regression coefficient of the wind onto the monsoon index M after linearly removing ENSO as in (3). For each monsoon index (IMI, WYI, and SAMI), we perform two perturbation experiments (see Figure 4), where M is equivalent to +1 and +2 standard deviations.

Acknowledgments

This work was supported by the Office of Science of the U.S. Department of Energy (DOE) Biological and Environmental Research as part of the Regional and Global Climate Modeling Program. The Pacific Northwest National Laboratory is operated for DOE by Battelle Memorial Institute under contract DE-AC05-76RL01830. The lead author is also grateful for encouragement from Peter Webster during an early phase of this work, and for constructive feedback from anonymous reviewers. Model simulations are publicly archived at https://figshare.com/articles/track_model_output_tar/7119503 and all other observational data are readily accessible from public repositories.

References

- Belanger, J. I., Curry, J. A., & Webster, P. J. (2010). Predictability of North Atlantic tropical cyclone activity on intraseasonal time scales. *Monthly Weather Review*, 138(12), 4362–4374. <https://doi.org/10.1175/2010MWR3460.1>
- Boudreault, M., Caron, L.-P., & Camargo, S. J. (2017). Reanalysis of climate influences on Atlantic tropical cyclone activity using cluster analysis. *Journal of Geophysical Research: Atmospheres*, 122, 4258–4280. <https://doi.org/10.1002/2016JD026103>
- Bove, M. C., Elsner, J. B., Landsea, C. W., Niu, X., & O'Brien, J. J. (1998). Effect of El Niño on U.S. landfalling hurricanes, revisited. *Bulletin of the American Meteorological Society*. [https://doi.org/10.1175/1520-0477\(1998\)079<2477:EOENOO>2.0.CO;2](https://doi.org/10.1175/1520-0477(1998)079<2477:EOENOO>2.0.CO;2)
- Chen, P., Hoerling, M. P., & Dole, R. M. (2001). The origin of the subtropical anticyclones. *Journal of the Atmospheric Sciences*, 58(13), 1827–1835. [https://doi.org/10.1175/1520-0469\(2001\)058<1827:TOOTSA>2.0.CO;2](https://doi.org/10.1175/1520-0469(2001)058<1827:TOOTSA>2.0.CO;2)
- Colbert, A. J., & Soden, B. J. (2012). Climatological variations in North Atlantic tropical cyclone tracks. *Journal of Climate*, 25(2), 657–673. <https://doi.org/10.1175/JCLI-D-11-00034.1>
- Compo, G. P., & Sardeshmukh, P. D. (2010). Removing ENSO-related variations from the climate record. *Journal of Climate*, 23(8), 1957–1978. <https://doi.org/10.1175/2009JCLI2735.1>
- Elsner, J. B. (2003). Tracking hurricanes. *Bulletin of the American Meteorological Society*, 84(3), 353–356. <https://doi.org/10.1175/BAMS-84-3-353>
- Elsner, J. B., & Bossak, B. H. (2001). Secular Changes to the ENSO–U.S. Hurricanes Relationship. *Geophysical Research Letters*, 28, 4123–4126. <https://doi.org/10.1029/2001GL013669>
- Elsner, J. B., Liu, K., & Kocher, B. (2000). Spatial variations in major U.S. hurricane activity: Statistics and a physical mechanism. *Journal of Climate*, 13(13), 2293–2305. [https://doi.org/10.1175/1520-0442\(2000\)013<2293:SVIMUS>2.0.CO;2](https://doi.org/10.1175/1520-0442(2000)013<2293:SVIMUS>2.0.CO;2)
- Emanuel, K., Ravela, S., Vivant, E., & Risi, C. (2006). A statistical deterministic approach to hurricane risk assessment. *Bulletin of the American Meteorological Society*, 87(3), 299–314. <https://doi.org/10.1175/BAMS-87-3-299>
- Goswami, B. N., Krishnamurthy, V., & Annamalai, H. (1999). A broad-scale circulation index for the interannual variability of the Indian summer monsoon. *Quarterly Journal of the Royal Meteorological Society*, 125(554), 611–633. <https://doi.org/10.1002/qj.49712555412>
- Gray, W. M. (1984). Atlantic seasonal hurricane frequency. Part I: El Niño and 30 mb Quasi-Biennial Oscillation influences. *Monthly Weather Review*. [https://doi.org/10.1175/1520-0493\(1984\)112<1649:ASHFPI>2.0.CO;2](https://doi.org/10.1175/1520-0493(1984)112<1649:ASHFPI>2.0.CO;2)
- Hall, T., & Yonekura, E. (2013). North American tropical cyclone landfall and SST: A statistical model study. *Journal of Climate*, 26(21), 8422–8439. <https://doi.org/10.1175/JCLI-D-12-00756.1>
- Holland, G. J. (1983). Tropical cyclone motion: Environmental interaction plus a beta effect. *Journal of the Atmospheric Sciences*, 40(2), 328–342. [https://doi.org/10.1175/1520-0469\(1983\)040<0328:TCMEIP>2.0.CO;2](https://doi.org/10.1175/1520-0469(1983)040<0328:TCMEIP>2.0.CO;2)
- Hurrell, J. W., Kushnir, Y., Otterson, G., & Visbeck, M. (2003). An overview of the North Atlantic Oscillation. In J. W. Hurrell, Y. Kushnir, G. Otterson, & M. Visbeck (Eds.), *The North Atlantic Oscillation: Climatic significance and environmental impact*, *Geophysical Monograph Series* (Vol. 134, pp. 1–35). Washington, DC: American Geophysical Union. <https://doi.org/10.1029/GM134>
- Ju, J., & Slingo, J. (1995). The Asian summer monsoon and ENSO. *Quarterly Journal of the Royal Meteorological Society*, 121(525), 1133–1168. <https://doi.org/10.1002/qj.49712152509>
- Kalnay, E., Kanamitsu, M., Kistler, R., Collins, W., Deaven, D., Gandin, L., et al. (1996). The NCEP/NCAR 40-year reanalysis project. *Bulletin of the American Meteorological Society*, 77(3), 437–471. [https://doi.org/10.1175/1520-0477\(1996\)077<0437:TNYRP>2.0.CO;2](https://doi.org/10.1175/1520-0477(1996)077<0437:TNYRP>2.0.CO;2)
- Kelly, P., Kravitz, B., Lu, J., & Leung, L. R. (2018). Remote drying in the North Atlantic as a common response to precessional changes and CO₂ increase over land. *Geophysical Research Letters*, 45, 3615–3624. <https://doi.org/10.1002/2017GL076669>
- Kelly, P., & Mapes, B. (2011). Zonal mean wind, the Indian monsoon, and July drying in the western Atlantic subtropics. *Journal of Geophysical Research*, 116, D00Q07. <https://doi.org/10.1029/2010JD015405>
- Kelly, P., & Mapes, B. (2013). Asian monsoon forcing of subtropical easterlies in the community atmosphere model: Summer climate implications for the western Atlantic. *Journal of Climate*, 26(9), 2741–2755. <https://doi.org/10.1175/JCLI-D-12-00339.1>

- Klotzbach, P. J. (2010). On the Madden-Julian Oscillation-Atlantic hurricane relationship. *Journal of Climate*, 23(2), 282–293. <https://doi.org/10.1175/2009JCLI2978.1>
- Kossin, J. P., Camargo, S. J., & Sitkowski, M. (2010). Climate modulation of North Atlantic hurricane tracks. *Journal of Climate*, 23(11), 3057–3076. <https://doi.org/10.1175/2010JCLI3497.1>
- Kozar, M. E., Mann, M. E., Camargo, S. J., Kossin, J. P., & Evans, J. L. (2012). Stratified statistical models of North Atlantic basin-wide and regional tropical cyclone counts. *Journal of Geophysical Research*, 117, D18103. <https://doi.org/10.1029/2011JD017170>
- Kumar, K. K., Rajagopalan, B., & Cane, M. A. (1999). On the weakening relationship between the Indian monsoon and ENSO. *Science*, 284(5423), 2156–2159. <https://doi.org/10.1126/science.284.5423.2156>
- Landsea, C. W. (1993). A climatology of intense (or major) Atlantic hurricanes. *Monthly Weather Review*, 121(6), 1703–1713. [https://doi.org/10.1175/1520-0493\(1993\)121<1703:ACOIMA>2.0.CO;2](https://doi.org/10.1175/1520-0493(1993)121<1703:ACOIMA>2.0.CO;2)
- Landsea, C. W., & Franklin, J. L. (2013). Atlantic hurricane database uncertainty and presentation of a new database format. *Monthly Weather Review*, 141(10), 3576–3592. <https://doi.org/10.1175/MWR-D-12-00254.1>
- Lee, J. Y., & Wang, B. (2014). Future change of global monsoon in the CMIP5. *Climate Dynamics*, 42(1-2), 101–119. <https://doi.org/10.1007/s00382-012-1564-0>
- Mo, K. C. (2000). The association between intraseasonal oscillations and tropical storms in the Atlantic basin. *Monthly Weather Review*, 128(12), 4097–4107. [https://doi.org/10.1175/1520-0493\(2000\)129<4097:TABIOA>2.0.CO;2](https://doi.org/10.1175/1520-0493(2000)129<4097:TABIOA>2.0.CO;2)
- Patricola, C. M., Chang, P., & Saravanan, R. (2016). Degree of simulated suppression of Atlantic tropical cyclones modulated by flavour of El Niño. *Nature Geoscience*, 9(2), 155–160. <https://doi.org/10.1038/ngeo2624>
- Patricola, C. M., Saravanan, R., & Chang, P. (2014). The impact of the El Niño-Southern Oscillation and Atlantic Meridional Mode on seasonal Atlantic tropical cyclone activity. *Journal of Climate*, 27(14), 5311–5328. <https://doi.org/10.1175/JCLI-D-13-00687.1>
- Pielke, R. A. J., & Landsea, C. W. (1999). La Nina, El Niño and Atlantic hurricane damages in the United States. *Bulletin of the American Meteorological Society*, 80(10), 2027–2033. [https://doi.org/10.1175/1520-0477\(1999\)080<2027:LNAENO>2.0.CO;2](https://doi.org/10.1175/1520-0477(1999)080<2027:LNAENO>2.0.CO;2)
- Rayner, N. A., Parker, D. E., Horton, E. B., Folland, C. K., Alexander, L. V., Rowell, D. P., et al. (2003). Global analyses of sea surface temperature, sea ice, and night marine air temperature since the late nineteenth century. *Journal of Geophysical Research*, 108(D14), 4407. <https://doi.org/10.1029/2002JD002670>
- Rodwell, M. J., & Hoskins, B. J. (1996). Monsoons and the dynamics of deserts. *Quarterly Journal of the Royal Meteorological Society*, 122(534), 1385–1404. <https://doi.org/10.1256/smsqj.53407>
- Rodwell, M. J., & Hoskins, B. J. (2001). Subtropical anticyclones and summer monsoons. *Journal of Climate*, 14(15), 3192–3211. [https://doi.org/10.1175/1520-0442\(2001\)014<3192:SAASM>2.0.CO;2](https://doi.org/10.1175/1520-0442(2001)014<3192:SAASM>2.0.CO;2)
- Shapiro, L. J. (1987). Month-to-month variability of the Atlantic tropical circulation and its relationship to tropical storm formation. *Monthly Weather Review*, 35(6), 533. [https://doi.org/10.1016/0198-0254\(88\)92448-X](https://doi.org/10.1016/0198-0254(88)92448-X)
- Shaw, T. A., & Voigt, A. (2015). Tug of war on summertime circulation between radiative forcing and sea surface warming. *Nature Geoscience*, 8(7), 560–566. <https://doi.org/10.1038/ngeo2449>
- Shukla, J., & Paolino, D. A. (1983). The southern oscillation and long-range forecasting of the summer monsoon rainfall over India. *Monthly Weather Review*, 111(9), 1830–1837. [https://doi.org/10.1175/1520-0493\(1983\)111<1830:TSOALR>2.0.CO;2](https://doi.org/10.1175/1520-0493(1983)111<1830:TSOALR>2.0.CO;2)
- Tang, B. H., & Neelin, J. D. (2004). ENSO influence on Atlantic hurricanes via tropospheric warming. *Geophysical Research Letters*, 31, L24204. <https://doi.org/10.1029/2004GL021072>
- Trenberth, K. E. (1997). The Definition of El Niño. *Bulletin of the American Meteorological Society*. [https://doi.org/10.1175/1520-0477\(1997\)078<2771:TDOENO>2.0.CO;2](https://doi.org/10.1175/1520-0477(1997)078<2771:TDOENO>2.0.CO;2)
- Vimont, D. J., & Kossin, J. P. (2007). The Atlantic Meridional Mode and hurricane activity. *Geophysical Research Letters*, 34, L07709. <https://doi.org/10.1029/2007GL029683>
- Waliser, D. E. (2006). Intraseasonal variability. *The Asian Monsoon*. https://doi.org/10.1007/3-540-37722-0_5
- Wang, B., & Fan, Z. (1999). Choice of South Asian summer monsoon indices. *Bulletin of the American Meteorological Society*, 80(4), 629–638. [https://doi.org/10.1175/1520-0477\(1999\)080<0629:COSASM>2.0.CO;2](https://doi.org/10.1175/1520-0477(1999)080<0629:COSASM>2.0.CO;2)
- Wang, B., Xiang, B., Li, J., Webster, P. J., Rajeevan, M. N., Liu, J., & et al. (2015). Rethinking Indian monsoon rainfall prediction in the context of recent global warming. *Nature Communications*, 6(1), 7154. <https://doi.org/10.1038/ncomms8154>
- Webster, P. J., & Yang, S. (1992). Monsoon and ENSO: Selectively interactive systems. *Quarterly Journal of the Royal Meteorological Society*, 118(507), 877–926. <https://doi.org/10.1002/qj.49711850705>
- Wu, L., & Wang, B. (2004). Assessing impacts of global warming on tropical cyclone tracks. *Journal of Climate*, 17(8), 1686–1698. [https://doi.org/10.1175/1520-0442\(2004\)017<1686:AIOGWO>2.0.CO;2](https://doi.org/10.1175/1520-0442(2004)017<1686:AIOGWO>2.0.CO;2)
- Xie, L., Yan, T. Z., Pietrafesa, L. J., Morrison, J. M., & Karl, T. (2005). Climatology and interannual variability of North American hurricane tracks. *Journal of Climate*, 18(24), 5370–5381. <https://doi.org/10.1175/JCLI3560.1>
- Zhao, H., Wu, L., & Zhou, W. (2009). Observational relationship of climatologic beta drift with large-scale environmental flows. *Geophysical Research Letters*, 36, L18809. <https://doi.org/10.1029/2009GL040126>